Reassessment of the intrinsic carrier density in crystalline silicon in view of band-gap narrowing

Pietro P. Altermatt
University of NSW, Centre for Photovoltaic Engineering, Sydney 2052, Australia and Inianga Consulting, 92/125 Oxford Street, Bondi Junction NSW 2022, Australia

Andreas Schenk and Frank Geelhaar
Integrated Systems Laboratory, ETH Zurich, Gloriastr. 35, 8092 Zurich, Switzerland

Gernot Heiser[a)]
University of NSW, Centre for Photovoltaic Engineering, Sydney 2052, Australia and University of NSW, School of Computer Science & Engineering, Sydney 2052, Australia

The commonly used value of the intrinsic carrier density of crystalline silicon at 300 K is $n_i = 1.00 \times 10^{10}$ cm^{-3}. It was experimentally determined by Sproul and Green, J. Appl. Phys. **70**, 846 (1991), using specially designed solar cells. In this article, we demonstrate that the Sproul and Green experiment was influenced by band-gap narrowing, even though the dopant density of their samples was low (10^{14} to 10^{16} cm^{-3}). We reinterpret their measurements by numerical simulations with a random-phase approximation model for band-gap narrowing, thereby obtaining $n_i = 9.65 \times 10^9$ cm^{-3} at 300 K. This value is consistent with results obtained by Misiakos and Tsamakis, J. Appl. Phys. **74**, 3293 (1993), using capacitance measurements. In this way, long-prevailing inconsistencies between independent measurement techniques for the determination of n_i are resolved. © *2003 American Institute of Physics.* [DOI: 10.1063/1.1529297]

I. INTRODUCTION

The intrinsic carrier density n_i is a fundamental quantity in semiconductor physics which enters almost all calculations that relate responses to excitations. For example, n_i strongly influences minority carrier densities and recombination properties. Therefore, the exact quantification of n_i is of prime importance for an improved understanding and design of semiconductor devices.

Prior to 1990, $n_i = 1.45 \times 10^{10}$ cm^{-3} was commonly used for crystalline silicon, leading to significant deviations between the theoretically predicted and the measured behavior of devices.[1] A value of $n_i = 1.08(8) \times 10^{10}$ cm^{-3} was suggested by Green[1] in 1990 (the digit in the parentheses represents the estimated one-standard-deviation uncertainty in the last digit of the previous value). Shortly thereafter, $n_i = 1.00(3) \times 10^{10}$ cm^{-3} was experimentally confirmed by Sproul and Green.[2,3] This is the most widely accepted value of n_i in the silicon community nowadays. Here, we reinterpret the Sproul and Green experiment by numerical simulations with a quantum-mechanical model for band-gap narrowing.[4] We obtain $n_i = 9.65(3) \times 10^9$ cm^{-3} at 300 K. This value is consistent with $n_i = 9.7(1) \times 10^9$ cm^{-3}, obtained by Misiakos and Tsamakis[5] using capacitance measurements. In this way, we resolve long-prevailing inconsistencies between independent measurements of n_i in crystalline silicon.

II. SPROUL AND GREEN EXPERIMENT

In their experiment, Sproul and Green fabricated p-n junction solar cells on high-purity float-zone (FZ) wafers. After an intentional degradation of the rear surface passivation, the external current of these cells was limited by the electron flow through the boron-doped base. Thus, the current-voltage (I–V) curves of these cells depended only on very few parameters: n_i, the mobility of minority electrons $\mu_{e,\min}$ in the base, the dopant density N_{dop} in the base, and the base thickness W. As $\mu_{e,\min}$, N_{dop}, and W were known from separate measurements of the same material, only n_i was unknown. Sproul and Green obtained n_i by reproducing their measured I–V curves with an analytical model, where n_i was adjusted as a free input parameter. Hence, their measurement technique is among the most direct methods of determining n_i.[1] The symbols in Fig. 1 show the measured dark I–V curves,[6,7] and the circles in Fig. 2 depict n_i extracted from these cells using the analytical model.[2,6] The error bars in Fig. 2 represent the one-standard-deviation uncertainty given by Sproul and Green.

III. REVISION OF BAND-GAP NARROWING

Figure 2 suggests that the Sproul and Green n_i values increase with rising dopant density. This tendency is weaker at other temperatures than 300 K (not shown here) because the Sproul and Green use of the Ebers–Moll theory implies a complex dependency on mobilities, which was most accurately incorporated at 300 K. Sproul and Green mentioned[6] that their measurements may be influenced by band-gap narrowing (BGN). This would imply that their data points in
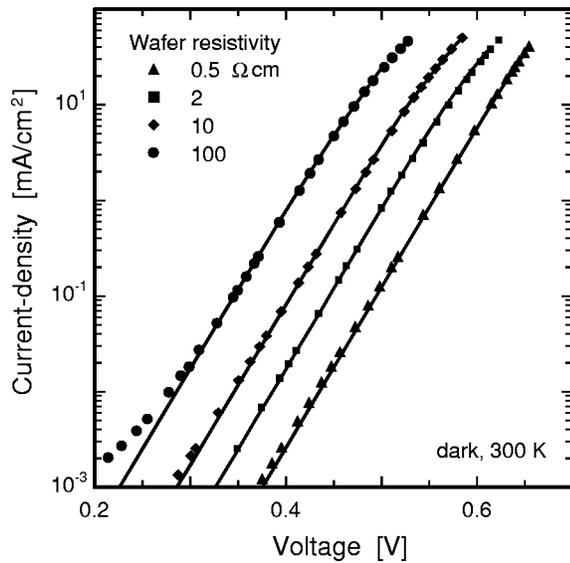
[a)]Electronic mail: g.heiser@unsw.edu.au

FIG. 1. Dark current-voltage ($I-V$) curves of specially designed silicon solar cells, measured by Sproul and Green (see Ref. 6) (symbols), and simulated using Dessis (see Ref. 65) with the BGN model of Ref. 4 (lines). These $I-V$ curves depend only on a very few material and device parameters, which were separately measured and hence enable the extraction of the intrinsic density shown in Fig. 2.

Fig. 2 do not represent n_i, but actually represent an effective intrinsic carrier density $n_{i,\mathrm{eff}}$ according to the formula

$$n_{i,\mathrm{eff}} = n_i e^{\beta \Delta E_g/2} \tag{1}$$

where $\Delta E_g > 0$ is the band gap narrowing and $\beta = 1/k_B T$ is the inverse thermal energy corresponding to an absolute temperature T. However, there were no measurements available in 1991 indicating BGN at $N_{\mathrm{dop}} < 2 \times 10^{17}$ cm^{-3}. Hence,
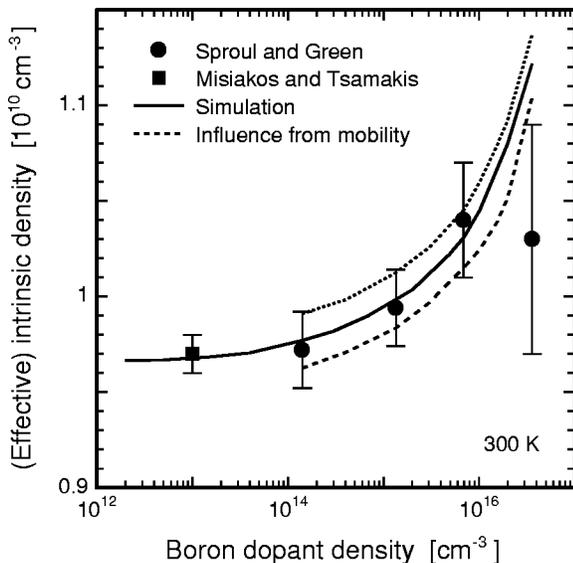
FIG. 2. The (effective) intrinsic carrier density of crystalline silicon, as a function of boron dopant density, determined by Sproul and Green (see Refs. 2 and 6) using their analytical model (circles), the value measured by Misiakos and Tsamakis (see Ref. 5) (square), and our simulations using $n_i = 9.65 \times 10^9$ cm^{-3} (solid line). The dashed lines represent our simulations using upper and lower-error bounds of the electron mobility (shown in Fig. 5).

Sproul and Green neglected BGN and interpreted the scattering of their data as inaccuracies of their measurement technique. They took the average of their n_i values as the outcome of their experiment to obtain $n_i = 1.00(3) \times 10^{10}$ cm^{-3}.

Meanwhile, Klaassen *et al.*[8] clarified the reasons why no BGN was detected at $N_A < 2 \times 10^{17}$ cm^{-3} in those days: The excessively high $n_i = 1.45 \times 10^{10}$ cm^{-3} was used in the data evaluation of the electrical BGN measurements. By means of Eq. (1), a value of n_i which is too high corresponds to a value of ΔE_g that is too low. Hence, the higher n_i is chosen, the higher is the minimal N_A where BGN will be detected. This is demonstrated in Figs. 3(a) and 3(b). Figure 3(a) shows the originally measured values of ΔE_g in p-type silicon,[8–12] where $n_i = 1.45 \times 10^{10}$ cm^{-3} was used in the data evaluation, and Fig. 3(b) shows a revision made by Klaassen *et al.*[8] using $n_i = 1.19 \times 10^{10}$ cm^{-3} of Green and Sproul (and revised mobility data). The work of Klaassen *et al.*[8] indicates a significant gap shrinkage ΔE_g in the doping range near 10^{16} cm^{-3}, as has been predicted before by theoretical considerations. The situation is similar in n type, as shown in Figs. 3(c)–3(e). This implies that indeed, the Sproul and Green experiment yields the effective intrinsic carrier density $n_{i,\mathrm{eff}}$ in Eq. (1) and not n_i itself. In this interpretation, the latter is given by the asymptotic value approached in the left part of Fig. 2. This will be demonstrated below.

So far, electronic devices have been mostly simulated with empirical parametrizations of BGN. Such parametrizations were derived from transport measurements in doped silicon and have been given as functions of the dopant density. There has been disagreement about which measuring method best yields BGN data relevant to device simulation. Figure 3 shows that the BGN values obtained by absorption measurements[13–20] are significantly smaller than those obtained by photoluminescence[21] or electronic techniques.[22,8–12,23–29] Like commonly experienced, we have applied the electronic BGN data most successfully to the simulation of solar cells and other electronic devices.[30] Since such BGN values scatter considerably, they yield no precise gap shrinkage at $N_{\mathrm{dop}} \approx 10^{16}$ cm^{-3}. Hence, we compute ΔE_g by means of Schenk's BGN model.[4] This model was derived within a full random-phase approximation (RPA) formalism for finite temperatures. The exchange-correlation self energy of the free carriers and the correlation energy of the carrier-dopant interaction were treated on an equal footing. The dispersive quasiparticle shift in RPA quality was calculated numerically. Based on these results, Padé approximations of the thermodynamically averaged, rigid band shifts $\Delta E_c = E_c^0 - E_c$ and $\Delta E_v = E_v - E_v^0$ were constructed in terms of the carrier and dopant densities and the temperature. $E_c^{(0)}$ and $E_v^{(0)}$ denote the intrinsic band-edge energies. The results of using this model for $\Delta E_g = \Delta E_c + \Delta E_v$ are depicted as solid lines in Fig. 3.

These ΔE_g values cannot be generally compared to the experimental BGN data derived from electrical measurements, shown as filled symbols in Fig. 3. This is so because the electrical BGN values were extracted from transport measurements, and are thus influenced by the transport
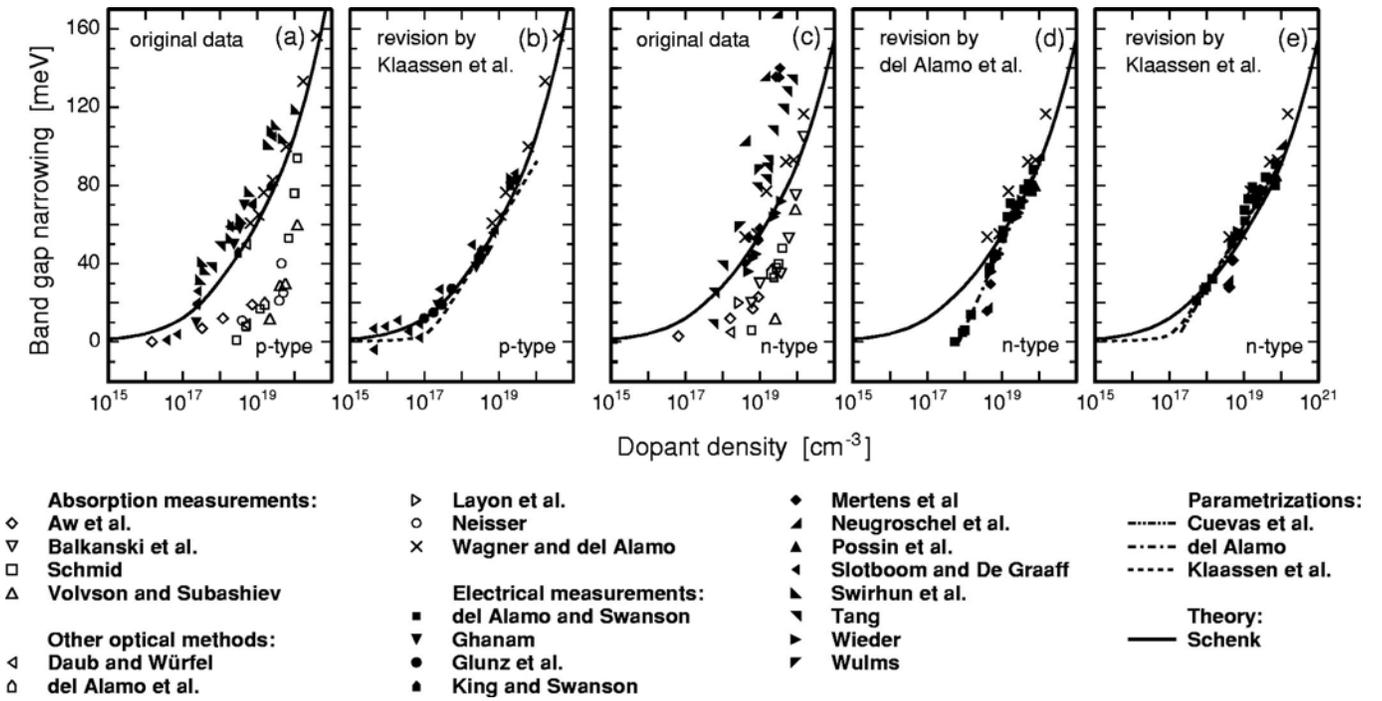
FIG. 3. Band-gap narrowing of crystalline *p*- and *n*-type silicon in low-injection and near 300 K. Depicted are absorption experiments (see Refs. 13–20) (open symbols), electrical measurements (see Refs. 8–12,22–29) (filled symbols), and photoluminescence measurements (see Ref. 67) (crosses). The lines represent the quantum-mechanical calculations of Ref. 4. Parametrizations, resulting from revisions of the n_i value and mobility, are also shown (see Refs. 8,28,68).

model employed in the data evaluation. In particular, Boltzmann statistics and the ideal density-of-states (DOS) of silicon were used, and it was furthermore assumed that $\Delta E_c = \Delta E_v$ (symmetric BGN). It has been theoretically shown, however, that the transport properties of free carriers are influenced by several factors: By degeneracy[31,32] at high-doping levels, by the change in DOS due to the formation of an impurity band[33] at medium–to–high dopant densities, and by the asymmetry of the gap shrinkage.[32–34] Since all these influences are neglected in the data evaluation of the empirical BGN values, the obtained values do not generally reflect the band-gap narrowing ΔE_g of Eq. (1), but are instead a conglomeration of various effects. Hence, they are referred to as an "apparent band gap narrowing" $\Delta E_g^{\mathrm{app}}$.

Since the Sproul and Green experiment was carried out at low-dopant densities and under low-level injection conditions, both carrier types were nondegenerate, and the DOS was essentially ideal. Reference 32 also shows that, under such conditions, the effects of asymmetry in BGN are unimportant. Thus, at low-dopant densities and under low-level injection conditions, the BGN theory of Ref. 4 can be directly compared with the experimental $\Delta E_g^{\mathrm{app}}$ values. Figure 3(b) shows that in *p* type, there is good agreement between the theory and electrical measurements in this case. In *n* type, there are no electrical BGN data available below $N_{\mathrm{dop}} = 5 \times 10^{17}$ cm^{-3}. This is not relevant to the Sproul and Green experiment, since the device parts having such low-phosphorus dopant densities are very small and do not influence the *I-V* curves. A recent study on *p*-type solar cells[22] experimentally confirmed the BGN theory of Ref. 4 in the doping range of $(1-4) \times 10^{17}$ cm^{-3}. Figures 3(b) and 3(e)

show that it also describes the experimental data at higher-dopant densities (up to 1×10^{19} cm^{-3}). For the reasons outlined above, the theory cannot be compared to the electrical measurements at $N_{\mathrm{dop}} > 1 \times 10^{19}$ cm^{-3}, but is most directly compared to photoluminescence measurements, shown as crosses. As expected, the theory yields slightly smaller BGN values than photoluminescence measurements because it neglects band tails.[35–37] Since band tails host immobile carriers and therefore do not contribute to BGN relevant to electronic devices, the theory describes the situation very well. The random-phase approximation underlying Schenk's model represents the first term in a diagrammatic expansion of the screened carrier self energies. In order to investigate the BGN due to higher-order terms, we calculated the plasma-induced band shift beyond the full RPA contribution Δ_a^{RPA} on the basis of the statically screened ladder approximation (SSLA).[38,39] This treatment corresponds to the Gould–DeWitt procedure[40] in plasma physics and incorporates both scattering and bound two-particle states. Focusing on the low–to–intermediate density range, we assumed Boltzmann statistics for simplicity. Details of the derivation can be found in Ref. 41. Here, we quote only the final result for a symmetric plasma of density $n_e = n_{\mathrm{h}}$,

$$\Delta_a = \Delta_a^{\mathrm{RPA}} - \frac{1}{\beta} \sum_b Z_{ab} \Lambda_{ab}^3 n_b + \frac{e^2}{4\pi\epsilon_{\mathrm{Si}}} \frac{\Lambda_{aa}^2 n_a}{2 g_a} \Phi\left(\frac{\kappa\lambda_{aa}}{2}\right)$$
$$+ \left(\frac{e^2}{4\pi\epsilon_{\mathrm{Si}}}\right)^2 \frac{\pi\beta}{\kappa} \sum_b \Phi\left(\frac{\kappa\lambda_{ab}}{2}\right) n_b, \qquad (2)$$

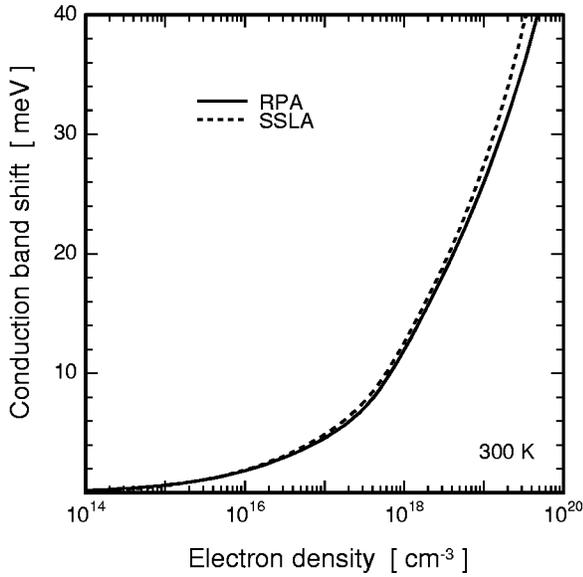where Z_{ab} denotes the interaction part of the two-body par-

FIG. 4. Comparison between the room-temperature conduction-band shift in Eq. (2) (solid line) and the RPA shift of Ref. 4 (dashed line). The contributions not covered by the RPA formalism can practically be neglected.
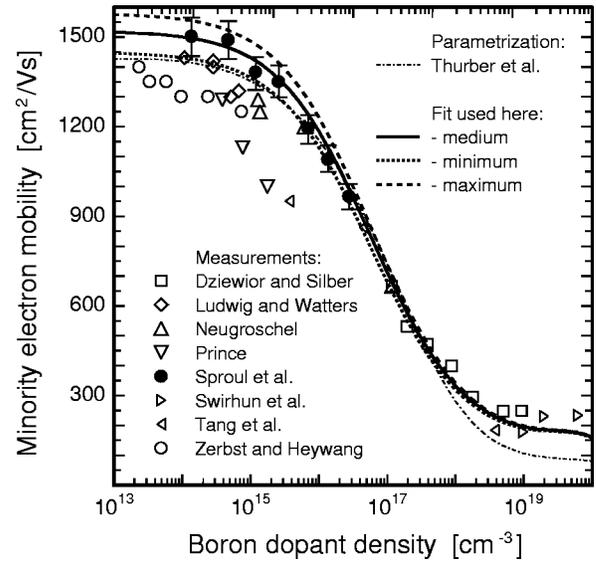

FIG. 5. The minority electron mobility at room temperature in boron-doped silicon, measured by various authors (see Refs. 11,47–53 (symbols), compared to a commonly used parametrization (see Ref. 54) and as introduced in this work by a modification of Klaassen's parametrization (see Ref. 64).

tition function[42,43] which is determined by the quantum-mechanical scattering phase shifts $\delta_{\ell,ab}(k)$ and binding energies $E_{n\ell} < 0$. These are obtained from the numerical solution of a radial Schrödinger equation with the static Debye interaction potential.[44,45] Furthermore, $\Lambda_{ab} = (4\pi)^{1/2}\lambda_{ab} = (2\pi\hbar^2/m_{ab})^{1/2}$ is the thermal wavelength, ϵ_{Si} the static dielectric constant, g_a the combined valley and spin degeneracy factor, and $\kappa^2 = (e^2\beta/\epsilon_{Si})\Sigma_b n_b$ the squared Debye screening wave number. We use the same material parameters as in Ref. 4. Note that in Eq. (2), the first correction term involving the function $\Phi(x) = 1 - \sqrt{\pi}x\exp(x^2)\text{erfc}(x)$ arises because the static Born scattering contribution is replaced by the dynamic RPA shift, while the second term takes into account that in the SSLA only direct self-energy diagrams with more than two interaction lines occur.

In Fig. 4, we compare the total conduction band shift Δ_e of Eq. (2) to Δ_e^{RPA} of Ref. 4. Evidently, for densities up to $n_e \approx 1 \times 10^{18}$ cm^{-3} their difference is negligibly small. Past this mark our assumption of nondegeneracy breaks down so that our curves for the band shift are no longer representative. In fact, the residual shift $\Delta_e - \Delta_e^{RPA}$ should tend to zero there, since it is known from the electron gas theory that Δ_e^{RPA} dominates the total quasiparticle shift in the high-density regime.[46] The situation is analogous for holes. Hence we conclude that at room temperature, Schenk's model adequately describes the plasma-induced BGN over the whole density range covered in our numerical simulations. Consequently, our extracted value for n_i should indeed reproduce the actual intrinsic carrier concentration within the given error bounds.

IV. MOBILITY MEASUREMENTS

The Sproul and Green $I-V$ curves are also influenced by the mobility of minority electrons in the base, $\mu_{e,\text{min}}$. We use the values given by Sproul et al.[47] who determined $\mu_{e,\text{min}}$ by photoconductance decay measurements of the same FZ sili-

con material as was used for the fabrication of the cells. Figure 5 shows that, in the doping range of $N_{\text{dop}} < 5 \times 10^{15}$ cm^{-3}, these $\mu_{e,\text{min}}$ values are higher than most measurements reported by other authors,[48–51,11,52,53] and also higher than the mobility of majority electrons $\mu_{e,\text{maj}}$ measured by Thurber et al.[54,55] It is expected that $\mu_{e,\text{min}} = \mu_{e,\text{maj}}$ in this doping range, because (i) the free carriers are mainly scattered by phonons, regardless of their charge, (ii) the drag effect is negligibly small at such low injection and dopant densities, and (iii) the difference in mobility data obtained from diffusivity or drift experiments are negligibly small. Hence, Fig. 5 shows a general discrepancy between the data of Sproul et al. and the values given by the other authors. This discrepancy arises mainly because the mobility is higher in FZ material than in Czochralski-grown (CZ) material. We discuss this topic at length in a separate paper[56] and outline our arguments here only shortly. In Fig. 6, we compare the data of Sproul et al.[47] and Thurber et al.[55] to the measurements of Litovchenko et al., who determined $\mu_{e,\text{maj}}$ in high-purity samples as well as in CZ samples containing $(5-8) \times 10^{17}$ cm^{-3} oxygen atoms.[57] Litovchenko's data, obtained from high-purity silicon, matches the FZ data of Sproul very well, while Litovchenko's CZ data coincides with Thurber's values. This indicates strongly that the different amounts of oxygen is the main reason why Sproul's mobility values, obtained in FZ material, are higher than Thurber's, obtained in CZ material. We cannot give ultimate reasons for these experimental findings. The scattering of electrons at the (neutral) oxygen atoms alone cannot reduce the mobility at 300 K substantially.[57,58] Other possible reasons for the mobility degradation include the electrical activity of defects induced by oxygen precipitation[59,60] and scattering at local phonon modes related to the oxygen precipitation.[61,62] The latter does not interfere with luminescence measurements indicating that phonon energies are insensitive to the oxygen density.[63] Litovchenko et al. derived
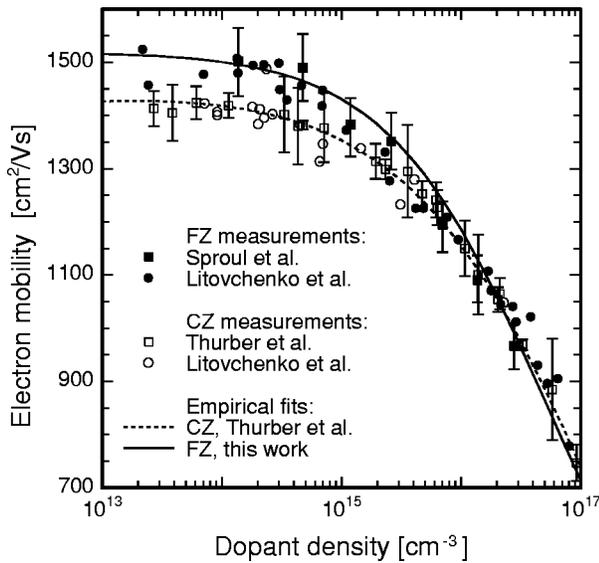
FIG. 6. At low-dopant densities, the electron mobility in float-zone (FZ) silicon is higher than in Czochralski-grown (CZ) silicon, as the comparison of various measurements (see Refs. 47,54,55,57) shows.

$\mu_{e,\mathrm{maj}}$ from Hall measurements, which we plot in Fig. 6 corrected as explained in our other publication.[56]

For the above reasons, the experiment of Sproul and Green needs to be simulated with the $\mu_{e,\mathrm{min}}$ values given by Sproul *et al.*[47] and not by Thurber *et al.* We assign Sproul's mobility values by adapting Klaassen's parametrization of mobility,[64] i.e., by increasing the electron mobility due to phonon scattering, μ_{L}, from 1414 to 1520 cm²/Vs. In order to account for the error estimates of Sproul's measurements, we introduce a fit through Sproul's upper and lower bounds by setting $\mu_L = 1580$ and 1450 cm²/Vs, respectively (see dashed lines in Fig. 5). The fit through the lower bounds lies very close to Thurber's parametrization of $\mu_{e,\mathrm{maj}}$ (dash-dotted line in Fig. 5).[54] Thurber's parametrization is most commonly utilized in device simulations, both for minority and majority carriers. In contrast, Klaassen's model applied here distinguishes between $\mu_{e,\mathrm{min}}$ and $\mu_{e,\mathrm{maj}}$. Since electrons scatter more efficiently at the P^+ ions than at the B^-

ions, $\mu_{e,\mathrm{min}}$ is larger than $\mu_{e,\mathrm{maj}}$ at $N_{\mathrm{dop}} > 5 \times 10^{17}$ cm⁻³, as shown in Fig. 5.

V. REEVALUATION OF THE SPROUL AND GREEN EXPERIMENT

To reproduce the Sproul and Green measured $I-V$ curves, we implement the BGN model of Ref. 4 in the device simulator Dessis[65] which numerically solves the fully coupled set of semiconductor differential equations in a self-consistent way. With an approach reported earlier,[66] we simulate the entire 2×2 cm² large cells of Sproul and Green, including 1 cm of wafer material surrounding the cells (which remained embedded in the wafer after fabrication). Our simulation parameters are listed in Table I.

The lines in Figs. 1 and 2 show our simulation results. We are able to reproduce all the measured $I-V$ curves in Fig. 1 very precisely using the (single) value of $n_i = 9.65 \times 10^9$ cm⁻³. These simulations underestimate the measured $I-V$ curves only at very low current-densities because shunt currents through the pn-junction are neglected. The simulated $n_{i,\mathrm{eff}}$ (solid line in Fig. 2) reproduces the apparent n_i values of Sproul and Green (symbols) very well, except at $N_A = 3.6 \times 10^{16}$ cm⁻³, where the analytical model of Sproul and Green may cause a systematic deviation. The dashed curves in Fig. 2 are obtained by using the error bounds of the mobility, i.e., $\mu_L = 1580$ and 1450 cm²/Vs, respectively (shown in Fig. 5). The error bounds in the mobility influence the extracted n_i only within the error bars given by Sproul and Green.

Misiakos and Tsamakis[5] measured n_i at carrier densities near 1×10^{13} cm⁻³, by means of capacitance measurements of p^+in^+ diodes, where the i layer had a n type dopant density of 4.5×10^{11} cm⁻³. They obtained a value of $9.7(1) \times 10^9$ cm⁻³, which is included in Fig. 2 (square). The error bar denotes the measurement uncertainty given by these authors. We plot their n_i value at a boron density of 1×10^{13} cm⁻³, because this is the injection density during their measurement, and the dopant type is irrelevant at such low dopant densities. Their n_i value is consistent with the Sproul and Green results for low N_A. In our interpretation,

TABLE I. Physical device parameters and models used in the numerical simulations.

Cell geometry	As published in Refs. 2 and 69
Perimeter region	1 cm from cell's edge[66]
Doping profile	As published in Refs. 2 and 69
Contact resistance	1×10^{-6} Ωcm, as given in Ref. 66
Temperature	300 K
Carrier statistics	Fermi–Dirac
Intrinsic carrier density	9.65×10^9 cm⁻³
Band-gap narrowing	Model of Ref. 4
Carrier mobility	Klaassen's model,[64] adapted to $\mu_L = 1520$ cm²/Vs
SRH recombination in bulk	Midgap defects with equal capture cross sections, lifetime τ as given in Ref. 2
SRH recombination at surface	Midgap defects with equal capture cross sections, $S = 600$ cm/s at the front[30]
SRH recombination at contacts	Ohmic, i.e., flat quasi-Fermi energy levels at midgap,[65,30] equivalent to $S = \infty$ cm/s
Auger recombination	Injection dependent model[70]

n_i is the asymptotic value towards low-dopant densities of the solid line in Fig. 2. This asymptotic value is consistent with measurements reported by both groups of authors, and is significantly lower than the average of the Sproul and Green data. As our simulations imitate the measurements of Sproul and Green, they cannot reduce the uncertainties of their technique. Hence, the one-standard-deviation uncertainty of n_i, extracted with our simulations, is at least 3%, the same that was given by Sproul and Green.

VI. CONCLUSIONS

We reinterpreted the n_i measurements of Sproul and Green on the basis of numerical simulations with a random phase approximation model of band-gap narrowing. Higher-order perturbation terms in the diagrammatic expansion of the screened carrier self energies were calculated in the statically screened ladder approximation and shown to give no significant contribution to BGN. We also critically revised and confirmed the minority-carrier mobility values used by Sproul and Green for the evaluation of their data. According to our interpretation, the Sproul and Green experiment was influenced by band gap narrowing although the dopant density in their samples was small. We conclude that the intrinsic carrier density n_i is given by the asymptotic value approached in the left part of Fig. 2. Hence, we find $n_i = 9.65 \times 10^9$ cm^{-3} in silicon at 300 K, a value which is consistent with the capacitance measurements performed by Misiakos and Tsamakis.

[1] M. A. Green, J. Appl. Phys. **67**, 2944 (1990).

[2] A. B. Sproul and M. A. Green, J. Appl. Phys. **70**, 846 (1991).

[3] A. B. Sproul and M. A. Green, J. Appl. Phys. **73**, 1214 (1993).

[4] J. Schenk, J. Appl. Phys. **84**, 3684 (1998).

[5] K. Misiakos and D. Tsamakis, J. Appl. Phys. **74**, 3293 (1993).

[6] A. B. Sproul, Ph.D. thesis, University of New South Wales, Sydney, Australia, 1992.

[7] In Ref. 2, the J_{sc}-V_{oc} curves were used. Reference 6 shows that the same n_i was obtained from the dark I-V curves.

[8] D. B. M. Klaassen, J. W. Slotboom, and H. C. de Graaff, Solid-State Electron. **35**, 125 (1992).

[9] R. R. King and R. M. Swanson, IEEE Trans. Electron. Devices **38**, 1399 (1991).

[10] J. W. Slotboom and H. C. de Graaff, Solid-State Electron. **19**, 857 (1976).

[11] S. E. Swirhun, Y. H. Kwark, and R. M. Swanson, *International Electronic Devices Meeting*, Los Angeles, CA (IEEE, New York, 1986), pp. 24–27.

[12] D. D. Tang, IEEE Trans. Electron Devices **27**, 563 (1980).

[13] S. E. Aw, H. S. Tan, and C. K. Ong, J. Phys.: Condens Matter **3**, 8213 (1991).

[14] M. Balkansi, A. Aziza, and E. Amzallag, Phys. Status Solidi **31**, 323 (1969).

[15] P. E. Schmid, Phys. Rev. B **23**, 5531 (1981).

[16] A. A. Volvson and V. K. Subashiev, Fiz. Tekh. Poluprovodn (S.Peterburg) (1967) [Semicond. **1**, 327 (1967)].

[17] E. Daub and P. Würfel, J. Appl. Phys. **80**, 5325 (1996).

[18] J. A. del Alamo, R. M. Swanson, and A. Lietoila, Solid-State Electron. **26**, 483 (1983).

[19] H. P. D. Lanyon, A. K. McCurdy, and R. A. Tuft, Proceedings of the 13th IEEE Photovoltaic Specialists Conference, Washington, D. C. (IEEE, New York, 1978), pp. 60–65.

[20] A. Neisser, "Spectral response measurements on silicon solar cells in the range of 1 eV to 5 eV photon energy at different temperatures," Master's thesis, Institut für Festkörperphysik, Technical University of Berlin, 1998.

[21] J. Wagner and J. A. del Alamo, J. Appl. Phys. **63**, 425 (1988).

[22] S. W. Glunz, J. Dicker, and P. P. Altermatt, Proceedings of the 17th EU Photovoltaic Energy Conference, Munich, Germany (WIP-Renewable Energies, Munich, Germany, 2001).

[23] R. P. Mertens, J. L. van Meerbergen, J. F. Nijs, and R. J. van Overstraeten, IEEE Trans. Electron Devices **27**, 949 (1980).

[24] A. Neugroschel, S. C. Pao, and F. A. Lindholm, IEEE Trans. Electron Devices **29**, 894 (1982).

[25] D. S. Lee and J. G. Fossum, IEEE Trans. Electron Devices **30**, 626 (1983).

[26] A. Wieder, IEEE Trans. Electron Devices **27**, 1402 (1980).

[27] H. E. J. Wulms, Solid-State Electron. **30**, 1127 (1987).

[28] J. del Alamo and R. M. Swanson, Solid-State Electron. **30**, 1127 (1987).

[29] G. E. Possin, M. S. Adler, and B. J. Baliga, IEEE Trans. Electron Devices **31**, 3 (1984).

[30] P. P. Altermatt, "The characterization and optimization of high-efficiency silicon solar cells by means of numerical simulations," Ph.D. thesis, University of Constance, Constance, Germany, 1997.

[31] F. A. Lindholm and J. G. Fossum, IEEE Electron Device Lett. **2**, 230 (1981).

[32] A. H. Marshak, M. Ayman-Shibib, J. G. Fossum, and F. A. Lindholm, IEEE Trans. Electron Devices **28**, 293 (1981).

[33] M. S. Lundstrom, R. J. Schwartz, and J. L. Gray, Solid-State Electron. **24**, 195 (1981).

[34] H. Kroemer, RCA Rev. **28**, 332 (1957).

[35] E. O. Kane, Solid-State Electron. **28**, 3 (1985).

[36] M. II. Cohen, M. Y. Chou, E. N. Ecoonomou, S. Jahn, and C. M. Soukoulis, IBM J. Res. Dev. **32**, 82 (1988).

[37] P. V. Mieghem, Rev. Mod. Phys. **64**, 755 (1992).

[38] H. Stolz and R. Zimmermann, Phys. Status Solidi B **B94**, 135 (1979).

[39] R. Zimmermann and H. Stolz, Phys. Status Solidi B **B131**, 151 (1985).

[40] H. A. Gould and H. E. DeWitt, Phys. Rev. **155**, 68 (1967).

[41] F. Geelhaar, "Quasi-excition densities and band-gap narrowing in bulk silicon at room temperature," Tech. Rep. 02/2002, Integrated Systems Laboratory, Swiss Federal Institute of Technology, Zurich, 2002.

[42] G. E. Uhlenbeck and E. Beth, Physica (Amsterdam) **3**, 729 (1936).

[43] E. Beth and G. E. Uhlenbeck, Physica (Amsterdam) **4**, 915 (1937).

[44] F. J. Rogers, H. C. Graboske, and D. J. Harwood, Phys. Rev. A **A1**, 1577 (1970).

[45] F. J. Rogers, Phys. Rev. A **A4**, 1145 (1971).

[46] R. Zimmermann, *Many-Particle Theory of Highly Excited Semiconductors* (BSB Teubner, Leipzig, Germany, 1988).

[47] A. B. Sproul, M. A. Green, and A. W. Stephens, J. Appl. Phys. **72**, 4161 (1992).

[48] J. Dziewior and D. Silber, Appl. Phys. Lett. **35**, 170 (1979).

[49] G. W. Ludwig and R. L. Watters, Phys. Rev. **101**, 1699 (1956).

[50] A. Neugroschel, IEEE Electron Device Lett. **6**, 425 (1985).

[51] M. B. Prince, Phys. Rev. **93**, 1204 (1954).

[52] D. D. Tang, F. F. Fang, M. Scheuermann, T. C. Chen, and G. Sai-Halasz, "Minority carrier transport in silicon," in *International Electronic Devices Meeting*, Los Angeles, CA (IEEE, New York, 1986), pp 20–23.

[53] M. Zerbst and W. Heywang, Z. Naturforsch. A **A11**, 608 (1956).

[54] W. R. Thurber, R. L. Mattis, Y. M. Liu, and J. J. Filiben, J. Electrochem. Soc. **127**, 1807 (1980).

[55] W. R. Thurber, R. L. Mattis, Y. M. Liu, and J. J. Filliben, "The relationship between resistivity and dopant density for phosphorous- and boron-doped silicon," 1981. U. S. National Bureau of Standards Special Publication 400-64.

[56] P. P. Altermatt, G. Heiser, and A. Schenk, J. Appl. Phys. (submitted, 2002).

[57] P. G. Litovchenko, V. S. Lutsyak, I. G. Kirnas, P. M. Kurilo, and V. M. Nitsovich, Phys. Status Solidi A **A21**, 419 (1974).

[58] A. Schenk, J. Appl. Phys. **79**, 814 (1996).

[59] T. Mchedlidze, K. Matsumoto, and E. Asano, Jpn. J. Appl. Phys. Pt. 1 **38**, 3426 (1999).

[60] J. Michel and L. C. Kimerling, *Semiconductors and Semimetals*, Vol. 42, pp. 251–287, 1994.

[61] F. Zeller, K. Lassmann, and W. Eisenmenger, Physica, B **263**, 108 (1999).

[62] M. D. McCluskey, J. Appl. Phys. **87**, 3593 (2000).

[63] M. Asche and O. Sarbei, Phys. Status Solidi B **103**, 11 (1981).

[64] D. B. M. Klaassen, Solid-State Electron. **35**, 953 (1992).

[65] S. Mueller, K. Kells, A. Benvenuti, J. Litsios, U. Krumbein, A. Schenk, and W. Fichtner, *Dessis 3.0 Manual* (Integrated Systems Engineering, Zurich, Switzerland, 1996).

[66] P. P. Altermatt, G. Heiser, A. G. Aberle, A. Wang, J. Zhao, S. J. Robinson, S. Bowden, and M. A. Green, Prog. Photovoltaics **4**, 399 (1996).

[67] J. Wagner and J. A. del Alamo, J. Appl. Phys. **63**, 425 (1988).

[68] A. Cuevas, P. A. Basore, G. Giroult-Matlakowski, and C. Dubois, J. Appl. Phys. **80**, 3370 (1996).

[69] A. Wang, "High efficiency PERL and PERC silicon solar cells," Ph.D. thesis, University of New South Wales, Sydney, Australia, 1992.

[70] P. P. Altermatt, J. Schmidt, G. Heiser, and A. G. Aberle, J. Appl. Phys. **82**, 4938 (1997).